



Chronic brain blood-flow imaging device for a behavioral experiment using mice

MAKITO HARUTA,^{1,5,*} YUKI KURAUCHI,^{2,5} MASAHIRO OHSAWA,³ CHIHIRO INAMI,³ RISAKO TANAKA,² KENJI SUGIE,¹ AYAKA KIMURA,¹ YASUMI OHTA,¹ TOSHIHIKO NODA,^{1,4} KIYOTAKA SASAGAWA,¹ TAKASHI TOKUDA,¹ HIROSHI KATSUKI,² AND JUN OHTA¹

¹Division of Materials Science, Graduate School of Science and Technology, Nara Institute of Science and Technology, 8916-5 Takayama, Ikoma-shi, Nara, Japan

²Department of Chemico-Pharmacological Sciences, Graduate School of Pharmaceutical Sciences, Kumamoto University, 5-1 Oe-honmachi, Chuo-ku, Kumamoto-shi, Kumamoto, Japan

³Department of Neuropharmacology, Graduate School of Pharmaceutical Sciences, Nagoya City University, 3-1 Tanabe-dori, Mizuho-ku, Nagoya-shi, Aichi, Japan

⁴Electronics-Inspired Interdisciplinary Research Institute, Toyohashi University of Technology, Hibarigaoka 1-1, Tempaku-cho, Toyohashi-shi, Aichi, Japan

⁵These authors contributed equally to this work.

*m-haruta@ms.naist.jp

Abstract: A chronic brain blood-flow imaging device was developed for cerebrovascular disease treatment. This device comprises a small complementary metal-oxide semiconductor image sensor and a chronic fiber-optic plate window on a mouse head. A long-term cerebral blood-flow imaging technique was established in a freely moving mouse. Brain surface images were visible for one month using the chronic FOP window. This device obtained brain surface images and blood-flow velocity. The blood-flow changes were measured in behavioral experiments using this device. The chronic brain blood-flow imaging device may contribute to determining the cause of cerebrovascular disease and the development of cerebrovascular disease treatment.

© 2019 Optical Society of America under the terms of the [OSA Open Access Publishing Agreement](#)

1. Introduction

In drug discovery and disease research, small experimental animals are used for the evaluation of treatments. However, long-term and repeated behavioral experiments with the same small experimental animal are difficult. A chronic window technique on the small animal brain was developed to solve this issue [1,2] and to enable repeated brain imaging with a living mouse. This technique implants a thin glass on the brain surface, allowing observation with an imaging microscope through the glass. However, this technique observes the brain surface of an anesthetized mouse or a head-fixed mouse. This technique does not use a behavioral experiment with a freely moving mouse. For a freely moving condition, an optical-fiber imaging technique [3,4] and a miniaturized microscope technique [5,6] were developed. These techniques realized chronic brain imaging. In previous studies, an implantable complementary metal-oxide semiconductor (CMOS) device was developed for blood-flow imaging, and an implantable micro imaging device was developed for deep-brain imaging [7–9]. These devices successfully obtained brain activities. However, the imaging area and imaging setup were not adjustable after implementation. In long-term experiments, the implanted device moved in the brain, and the imaging area was obstructed. Additionally, these devices [10,11] did not observe brain-surface images for a long time, because the structures of the devices damaged the brain surface. In this study, a blood-flow imaging device was developed for long-term and repeated behavioral experiments with the same small experimental animal. Blood-flow imaging was performed in the sensory cortex of a mouse

with a small CMOS imaging device. Brain activities and blood flow are closely related. Blood flow and vessels are highly interested in brain studies [12–14]. In this study, this device was used to measure blood flow for a long time, because the device required no staining for optical imaging. Blood-flow imaging can be used in clinical applications, because it requires no staining and is minimally invasive. The absorption spectrum of the hemoglobin in the blood was used. The illumination wavelength was 535 nm, effectively absorbed by hemoglobin [15,16]. The result of this study could contribute to the understanding of blood-flow systems in the brain related to drug potency for diseases.

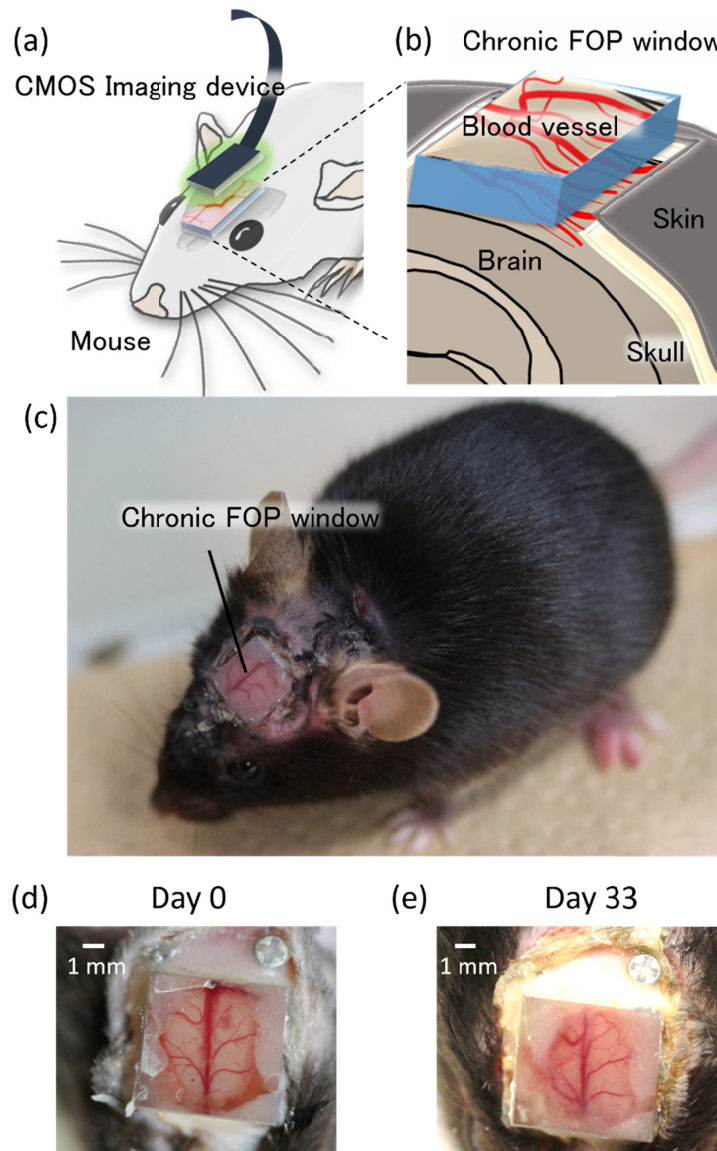


Fig. 1. Chronic brain blood-flow imaging device for a behavioral experiment using mice. (a) shows the outline of the device, and (b) shows the chronic FOP window on the brain surface. (c) shows a picture of the mouse that has the chronic FOP window on its head. (d) shows a picture that captured in the day of surgery. (e) shows a picture that was captured in the 33th day after surgery.

2. Materials and methods

2.1 Chronic brain blood-flow imaging device for the cerebral blood flow of the mouse

The chronic brain blood-flow imaging device was developed for long-term mouse cerebral blood-flow measurement in a behavioral experiment. See Fig. 2(a). This device includes a CMOS image sensor, green light-emitting diode (LED) for light sources, and a fiber-optic plate (FOP) on a flexible printed circuit (FPC) (TAIYO INDUSTRIAL CO., Japan) in Fig. 2(b). The CMOS image sensor was designed and fabricated using the standard CMOS process (0.35- μm , 2-poly-4 metal CMOS; Austria Microsystems, Austria). The pixel size of the CMOS image sensor was $7.5 \times 7.5 \mu\text{m}$, and this sensor held 120×268 pixels. This device had six green LEDs (EPISTAR Corp., Taiwan) with an emission wavelength of 535 nm, located around the sensor as light sources. This wavelength is one of the absorption spectral peaks of hemoglobin in the blood. At this wavelength, blood flow is measured from the hemoglobin in the blood vessels. The LED size was $280 \times 300 \mu\text{m}$. Parts of the device were connected to other parts using a wire-bonding tool. Finally, an FOP (Hamamatsu Photonics, Japan) was mounted on the component side of the CMOS image sensor and LEDs. In this study, we used a high-resolution FOP J5734. The FOP is comprised of a bundle of micron-sized optical fibers. The diameter of the optical fiber was $3 \mu\text{m}$. An incident image from an end face of the FOP was transmitted to the opposite side of the FOP. The FOP had the same optical quality as an optical fiber bundle for image transmission. In this study, alignment of FOP and CMOS was less affected, because the resolution of the CMOS image sensor ($7.5 \mu\text{m}$) was much larger than the resolution of the FOP ($3 \mu\text{m}$). In this study, we used a surface irradiation CMOS image sensor. When we mounted the sensor on the substrate, we wire-bonded the same surface of the CMOS image sensor. However, the CMOS image sensor did not closely attach to the chronic FOP window, because the imaging surface was not flat by the bonding wire. Therefore, we put the FOP on the pixel array area of the image sensor to make a flat surface. The FOP raises the imaging surface higher than the wire-bonding area. Because of this structure, the chronic brain blood-flow imaging device captured a clear brain surface image with a high spatial resolution and light intensity. Black paint was used to shield the side of the device (CANON CHEMICALS INC., Japan). The weight of the device was 0.40 g, 1/50 of an adult mouse. The power of the LED was 50–100 mW/mm. We adjusted light power for each experiment. The illumination uniformity was obtained by arranging 6 LEDs around the CMOS image sensor. The LED light was scattered onto the brain surface, because the brain tissue is a light-scattering material.

The input and output signals of the image sensor were transmitted to a control board through a small relay board using four wires. The relay board contained an operational amplifier and a digital buffer used to regenerate the attenuated signals. The light intensity was controlled using a current generator through a small relay board. The control board included a digital–analog converter for transmitting signals to a personal computer (PC), because the sensor output contained analog signals. The analog output signals transmitted from the sensor were converted to 14-bit digital data. All the signals were controlled using an original PC program. In this experiment, the images were stored in the PC. Maximum frame rate was 120 Hz.

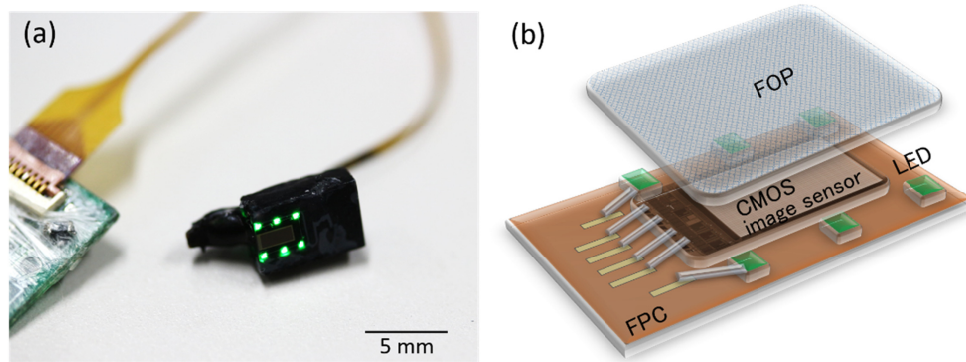


Fig. 2. Structure of the chronic brain blood-flow imaging device. (a) shows a picture of the chronic brain blood-flow imaging device. The device illuminated the LEDs ($\lambda = 535$ nm). (b) shows the structure of the device. This device includes the CMOS image sensor, six green LEDs, and a FOP on an FPC.

2.2 Chronic FOP window for the chronic brain blood-flow imaging device

A chronic FOP window was developed for long-term brain-surface imaging. A common chronic window uses thin glass for the window of the brain surface. However, chronic brain blood-flow imaging devices cannot use the common chronic window. Because this imaging device does not have optical components, such as an optical lens, the brain-surface image is out of focus using this window. In this study, the FOP was used for the chronic window. The FOP was made of glass optical fiber, and the fibers were bundled into a flat plate. The structure of the FOP was used as the chronic window on the mouse brain surface. Our CMOS imaging device maintained the spatial resolution by using this FOP, because its resolution was higher than that of the CMOS image sensor. The CMOS image sensor can capture clear brain-surface images without direct contact to the surface. The size of the chronic FOP window was $6.78 \times 6.86 \times 2.54$ mm. The weight of the chronic FOP window was 0.45 g. The core diameter of the FOP fiber was $3 \mu\text{m}$.

2.3 Animal preparation

C57BL/6 mice (SLC Co., Japan, 7–10 weeks of age, 20–25 g) were used in this study. All animal procedures conformed to the animal care and experimentation guidelines of the Nara Institute of Science and Technology. A combination anesthetic that was prepared with 0.75 mg/kg of medetomidine, 4.0 mg/kg of midazolam, and 5.0 mg/kg of butorphanol was introduced into the abdominal cavity of the mouse using a syringe [17]. The mouse head was fixed in a stereotaxic instrument (Narishige). The body of the mouse was kept warm by a heater. The skull of the mouse was exposed and cleaned, and the primary sensory cortex was observed (posterior 0.5 mm and lateral 2.5 mm). A craniotomy (less than 10-mm square) was performed above the observed region. The center of the craniotomy was positioned above the sensory cortex in an area corresponding to the frontal and hind limb regions. Next, the chronic FOP window was constructed on the brain surface, as shown in Fig. 1(b). The FOP was placed on the brain surface, and the anchors were set with stainless micro screws onto the skull around the FOP after the craniotomy. Finally, the FOP was fixed using dental cement between the skull and anchors. Figure 1(c) shows a picture of a mouse with the chronic FOP window on the head. For putting the CMOS imaging device on the chronic FOP window, we determined the position of the CMOS imaging device on the chronic FOP window by the shape of the blood vessels on the brain surface. Finally, we fixed the device to the chronic FOP window using the dental cement.

2.4 Blood-flow imaging and behavioral experiment

The blood-flow changes in the brain were obtained from changes in the reflection of the green light using the pixel value in the CMOS image sensor. The pixel-value data, stored in the PC, were analyzed by an original program written using Matlab. In the blood-flow velocity analysis, the velocity was shown as segments of the line scan along the blood vessel, plotted over time. The dark stripes corresponded to the red blood cells traveling along the length of the vessel, and the slope of the lines was proportional to the speed at which the hemoglobin traveled. We prepared the line-scan image with the distance, x (mm), of the measured blood vessel on the abscissa at time, t (s), of the scan of the ordinate. We calculated blood-flow velocity, V (mm/s), from $V = x/\Delta t$. Δt is the changing time of the slope of the line-scan image. We detected 10 lines from the line-scan image and calculated the average of the blood flow velocity (mm/s) from 10 lines. The range of detection of blood-flow velocity depends on the frame rate of the CMOS image sensor. Our image sensor operates within 1 to 120 fps. The range of the detection was 0.075 to 15 mm/s (measurement pixel number: 50; measurement frame number: 200). After obtaining the line-scan data, the data in the longitudinal area and the lateral lines were averaged to remove noise.

For brain-activity measurement, the device measured brightness changes of the brain surface. Capillary blood vessels were not obtained, running throughout the brain surface. When brain activities occur, blood-flow volume of capillary blood vessels is increased temporarily for delivering sustenance and oxygen to neurons. In this experiment, we show the result of this. The value of Fig. 6(a) indicates the average of the pixel value rate (%) of the mean value, R , of the ROI (9×9 pixels). The pixel value rate was calculated from $\Delta R/R_0$. R_0 is the average value of the ROI in measurement time. ΔR was calculated from $R - R_0$.

3. Results

3.1 Conditions of the mouse cerebral surface with the chronic real-time imaging system

We observed conditions of the brain surface through the chronic FOP window after implantation. Figures 1(d) and (e) show pictures of the chronic FOP window captured on the day of surgery and 33 days afterwards. The brain surface kept good conditions one month afterwards. The chronic FOP window demonstrated use in long-time stable conditions.

Figures 3(a) and (b) show the brain-surface images captured by a commercial camera. The brain surface had a small hemorrhage on the edge. However, the observation area had no damage, and the blood vessels were in good condition. The chronic FOP window had no effect on mouse behavior. The imaging device observed the same brain surface area in Fig. 3(c). The blood vessels appeared as black lines in this image, because the green light was effectively absorbed by the hemoglobin in the red blood cells.

In Fig. 4, the blood-flow velocity was measured with an imaging device. We set the device to a frame rate 66.41 fps and an exposure time 15.06 ms. The blood-flow velocity was analyzed by subtracting the images and the line scan images. In [Visualization 1](#), the subtracted images made from the brain surface images. The blood flow was observed. An analysis of the blood-flow velocity was performed in a part of the line, as shown in Fig. 4(a). The results of the line scan are shown in Fig. 4(b). The direction of the slope was the direction of the blood flow, and the estimate of the slope shows the blood-flow velocity. The results of the blood-flow velocity are shown in Fig. 4(b). The blood-flow velocities of the vessel were estimated, as shown in Fig. 4(b). The velocities were 0.88 mm/s, 1.13 mm/s, and 1.22 mm/s.

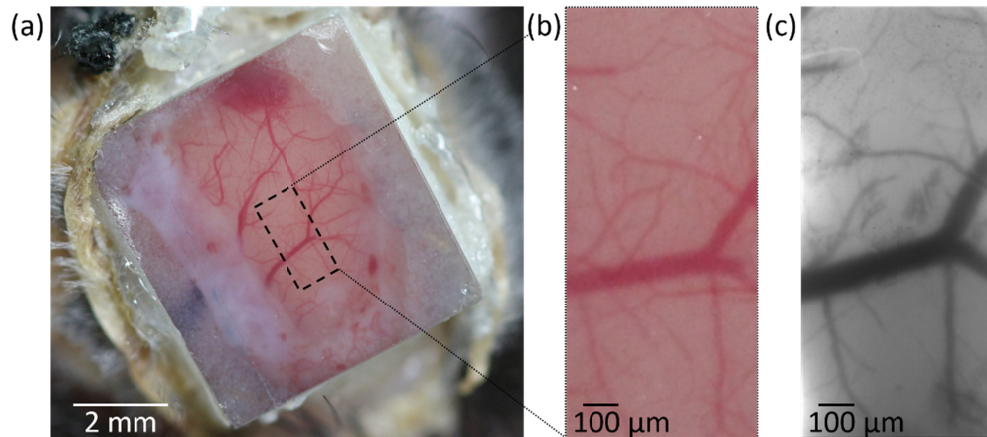


Fig. 3. Brain-surface images with the chronic FOP window. (a) shows the chronic FOP window on the mouse head. The brain surface was observed clearly through the chronic FOP window. The part surrounded by the block dotted lines indicates the imaging area of the device. (b) shows the imaging area of the device captured by a microscope. (c) shows the brain surface image captured by the device with a green light source. The black lines are blood vessels.

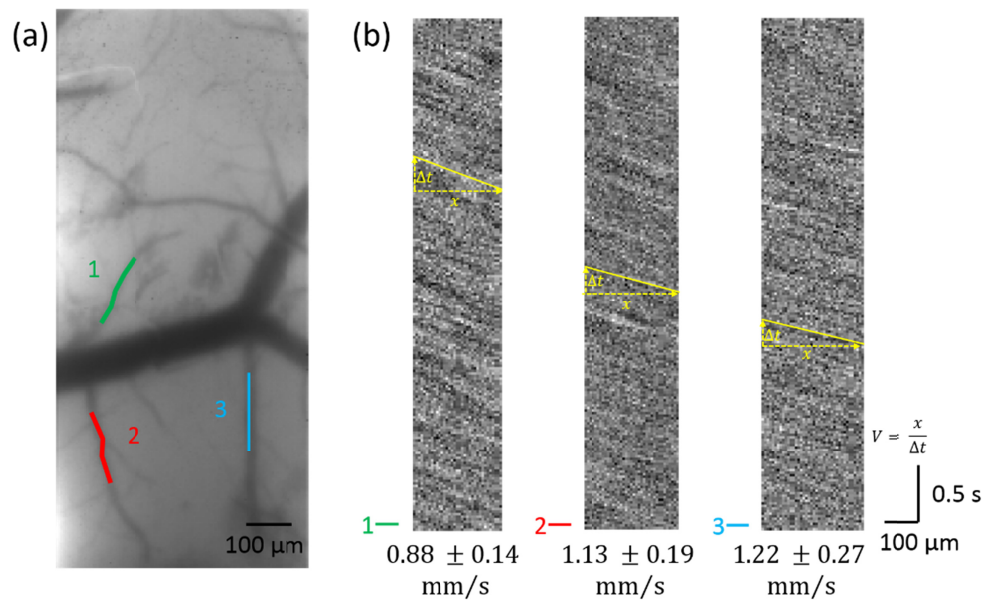


Fig. 4. Results of the blood-flow measurement with the chronic brain blood-flow imaging device and the chronic FOP window. (a) shows the brain surface image captured by the device (see Visualization 1). The green line, red line, and blue line indicate the measurement areas of the blood vessels. (b) shows the results of the line scans of the blood vessels. The slopes of the diagonal lines indicate the blood-flow velocity. The mean of the blood flow velocity was calculated from 10 lines in each line-scan result.

3.2 Mouse cerebral blood-flow imaging with the chronic brain blood-flow imaging device in a freely moving experiment

For the freely moving experiment, a chronic FOP window and a guide cannula in the mouse head were implanted, as shown in Fig. 5(a). The guide cannula was implanted in the visual cortex. After waiting 3 days for the mouse to recover, the blood flow was observed on the

brain surface. In this experiment, the blue light illuminated the experimental setup, as shown in Fig. 5(b). The blue light did not penetrate into the skin and tissues. Therefore, this setup enabled observation of blood flow in the behavioral experiments using tracking videos. First, the blood flow was measured on the brain surface with an imaging device. In Figs. 5 and 6, we set the device to frame rate 110.64 fps and exposure time 9.04 ms. Figure 5(c) shows a brain-surface image captured in the freely moving experiment by the device. The result of a blood-flow measurement is shown in Fig. 5(d). The imaging device obtained the measured blood-flow velocities in the behavioral experiments. The velocities were 1.32 and 0.72 mm/s.

Second, the brain activity on the brain surface was measured by neural stimulation. A 1-M, 10- μ L KCl solution was injected into the visual cortex using the cannula in Fig. 5(a). This stimulation elicited propagation of Ca^{2+} signals in the brain, and this propagation changed the brain activity at the brain surface. After injection, the brain activity on the sensory cortex area were obtained by the imaging device, as shown in Figs. 6(b) and 6(c). Figure 6(a) shows the brain surface. The five parts surrounded by square lines are the measurement areas that measured the light intensity in Fig. 6(c). Figure 6(c) shows light intensity profiles. The brain activity changes were transmitted from point 1 to point 5. In [Visualization 2](#), the blood-flow changes are shown.

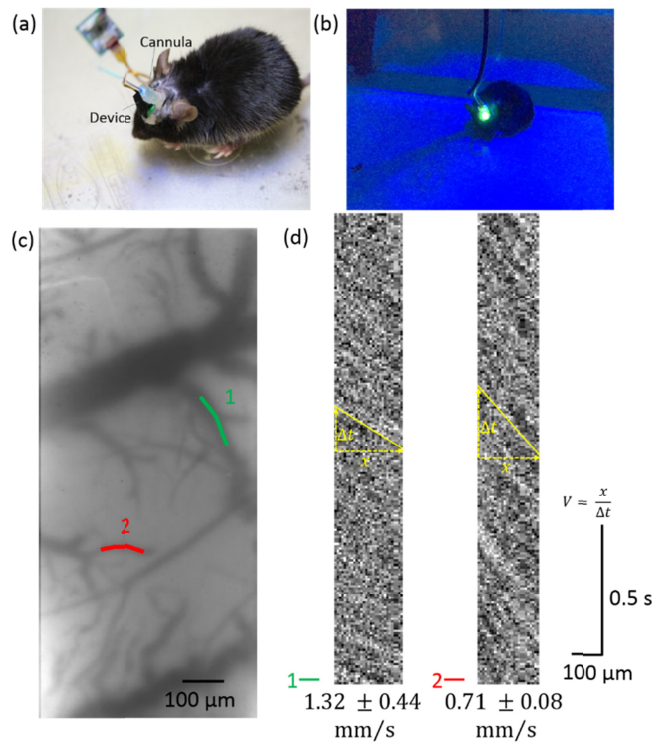


Fig. 5. Cerebral blood flow imaging in a freely moving experiment. (a) shows a picture of a mouse with the chronic brain blood-flow imaging device and chronic FOP window. In this experiment, a cannula was used to stimulate the brain activity. (b) shows a picture of the behavioral experiment with the mouse. The green LED light source of the device was illuminated. A blue illumination light was used for this experiment, because the blue light did not penetrate the skin and tissues. (c) shows the brain surface image captured in the freely moving experiment by the device. (d) shows the line-scan image obtained in the freely moving experiment.

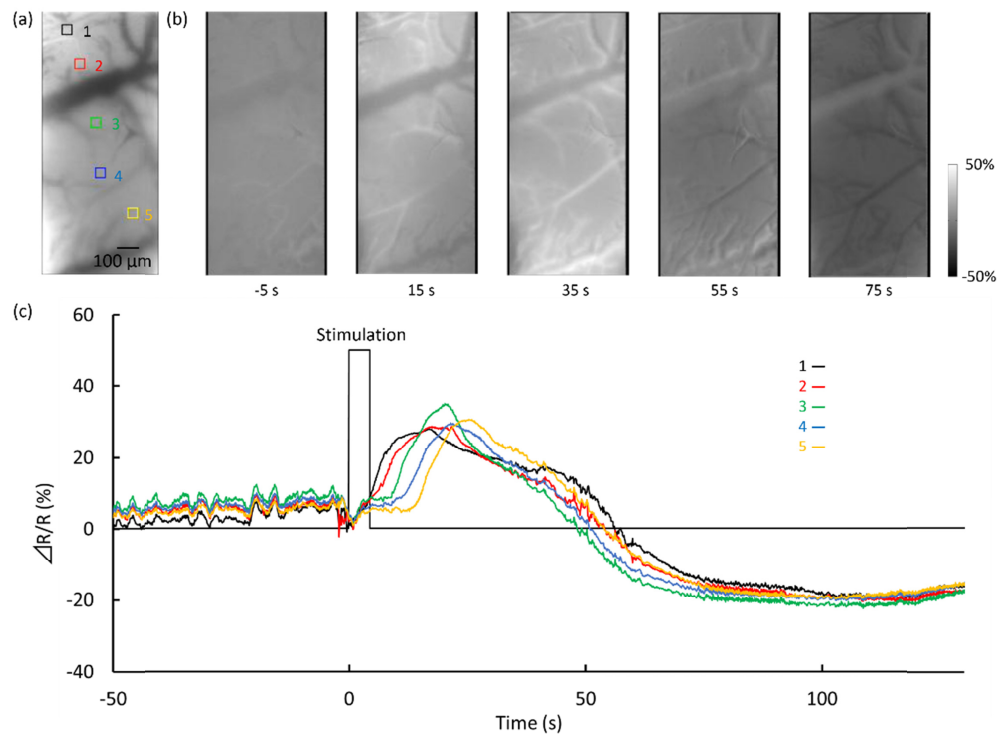


Fig. 6. Measurement results of the brain activity changes in the brain surface in the freely moving experiment. (a) shows the brain surface image captured by the device. The five parts surrounded by square lines indicate the measurement areas of the changing signals. (b) shows the time-lapsed images of the brain activity changes in the brain surface with stimulation (see [Visualization 2](#)). (c) shows the graph of the brain activity changes at the brain surface. The brain activity changes were transmitted from point 1 to point 5.

4. Discussion

Measuring long-term cerebral blood flow was difficult using the implantable CMOS device was developed in our previous study [10,11], because animal movement and tissue inflammation led to bleeding on the brain surface. Therefore, a chronic FOP window technique was developed to achieve long-term cerebral blood-flow imaging in a mouse behavioral experiment. The chronic FOP window technique produced minimal damage to the brain, because it used a method similar to that of a typical chronic window technique with glass [1]. The main ingredient of the FOP is glass. The FOP is not toxic. In this study, clear brain surface images were observed through the FOP window one month after implantation. The FOP window was minimally invasive. This a good behavioral experiment. This achievement enables the measurement of blood flow for psychiatric and cerebrovascular diseases [18–20]. In the blood-flow imaging methods, the imaging speed and analysis program were improved. The imaging speed was upgraded to 120 fps, greater than the maximum frame rate of 58 fps in the previous study. The analysis program measured the blood-flow velocity from a curved blood vessel. These upgrades expanded the versatility of this chronic brain blood-flow imaging device. The CMOS imaging device can detect blood flow velocity from a tiny blood vessel with a diameter under 7.5 μm with blood flow.

In the cerebral blood-flow imaging experiment, the blood flow was measured in the freely moving experiment, and the blood-flow velocity was obtained from multiple blood vessels. In this experiment, the brain activities were measured using the device. The blood-flow changes—related to brain activities in the sensory cortex—were obtained after stimulation.

This device could simultaneously measure the blood-flow velocity and brain activity. These results suggested that the chronic brain blood-flow imaging device could be used for the development of a therapeutic methods for cerebrovascular disease [21]. The treatment effect and recovery process applying to cerebrovascular disease could also be determined by the devices ability to provide long-term observation in a freely moving experiment.

5. Conclusion

A chronic brain blood-flow imaging device was developed, and blood-flow measurement was demonstrated in a freely moving experiment using a mouse. This device comprised a small image sensor based on CMOS integrated circuit technology and a chronic FOP window on the mouse head. The chronic brain blood-flow imaging device obtained the blood-flow velocity of the cortex through the chronic FOP window. The chronic brain blood-flow imaging device observed clear brain surface images through the chronic FOP window 1 week after implantation. The blood-flow velocity and brain activity were obtained in the freely moving experiment using the device. The chronic brain blood-flow imaging device performed long-term brain imaging. The device can be used in long-term behavioral experiments for the development of therapeutic methods for treating cerebrovascular disease. The advantages of this device include its usefulness for experimentation, such as drug discovery research and disease research.

Funding

Japan Society for the Promotion of Science (JSPS) (18H03780, 16K16652, 17K15458, 16H05460).

Acknowledgments

This study was supported by the VLSI Design and Education Center (VDEC), the University of Tokyo in collaboration with the Cadence Corporation and Mentor Graphics Corporation.

Disclosures

The authors declare that there are no conflicts of interest related to this article.

References

1. A. Holtmaat, T. Bonhoeffer, D. K. Chow, J. Chuckowree, V. De Paola, S. B. Hofer, M. Hübener, T. Keck, G. Knott, W. C. Lee, R. Mostany, T. D. Mrsic-Flogel, E. Nedivi, C. Portera-Cailliau, K. Svoboda, J. T. Trachtenberg, and L. Wilbrecht, "Long-term, high-resolution imaging in the mouse neocortex through a chronic cranial window," *Nat. Protoc.* **4**(8), 1128–1144 (2009).
2. T. H. Kim, Y. Zhang, J. Lecoq, J. C. Jung, J. Li, H. Zeng, C. M. Niell, and M. J. Schnitzer, "Long-Term Optical Access to an Estimated One Million Neurons in the Live Mouse Cortex," *Cell Reports* **17**(12), 3385–3394 (2016).
3. K. K. Ghosh, L. D. Burns, E. D. Cocker, A. Nimmerjahn, Y. Ziv, A. E. Gamal, and M. J. Schnitzer, "Miniaturized integration of a fluorescence microscope," *Nat. Methods* **8**(10), 871–878 (2011).
4. W. Zong, R. Wu, M. Li, Y. Hu, Y. Li, J. Li, H. Rong, H. Wu, Y. Xu, Y. Lu, H. Jia, M. Fan, Z. Zhou, Y. Zhang, A. Wang, L. Chen, and H. Cheng, "Fast high-resolution miniature two-photon microscopy for brain imaging in freely behaving mice," *Nat. Methods* **14**(7), 713–719 (2017).
5. I. Ferezou, S. Bolea, and C. C. H. Petersen, "Visualizing the cortical representation of whisker touch: voltage-sensitive dye imaging in freely moving mice," *Neuron* **50**(4), 617–629 (2006).
6. J. H. Jennings, R. L. Ung, S. L. Resendez, A. M. Stamatakis, J. G. Taylor, J. Huang, K. Veleta, P. A. Kantak, M. Aita, K. Shilling-Scriver, C. Ramakrishnan, K. Deisseroth, S. Otte, and G. D. Stuber, "Visualizing Hypothalamic Network Dynamics for Appetitive and Consummatory Behaviors," *Cell* **160**(3), 516–527 (2015).
7. J. Ohta, T. Tokuda, K. Sasagawa, and T. Noda, "Implantable CMOS Biomedical Devices," *Sensors (Basel)* **9**(11), 9073–9093 (2009).
8. A. Tagawa, A. Higuchi, T. Sugiyama, K. Sasagawa, T. Tokuda, H. Tamura, Y. Hatanaka, Y. Ishikawa, S. Shiosaka, and J. Ohta, "Development of Complementary Metal Oxide Semiconductor Imaging Devices for Detecting Green Fluorescent Protein in the Deep Brain of a Freely Moving Mouse," *Jpn. J. Appl. Phys.* **48**, 04C195 (2009).

9. Y. Sunaga, H. Yamaura, M. Haruta, T. Yamaguchi, M. Motoyama, Y. Ohta, H. Takehara, T. Noda, K. Sasagawa, T. Tokuda, Y. Yoshimura, and J. Ohta, "Implantable imaging device for brain functional imaging system using flavoprotein fluorescence," *Jpn. J. Appl. Phys.* **55**(3S2), 3S2 (2016).
10. M. Haruta, C. Kitsumoto, Y. Sunaga, H. Takehara, T. Noda, K. Sasagawa, T. Tokuda, and J. Ohta, "An implantable CMOS device for blood-flow imaging during experiments on freely moving rats," *Jpn. J. Appl. Phys.* **53**(4S), 04EL05 (2014).
11. M. Haruta, Y. Sunaga, T. Yamaguchi, H. Takehara, T. Noda, K. Sasagawa, T. Tokuda, and J. Ohta, "Intrinsic signal imaging of brain function using a small implantable CMOS imaging device," *Jpn. J. Appl. Phys.* **54**(4S), 04DL10 (2015).
12. D. Wang, J. Qian, W. Qin, A. Qin, B. Z. Tang, and S. He, "Biocompatible and photostable AIE dots with red emission for in vivo two-photon bioimaging," *Sci. Rep.* **4**(1), 4279 (2015).
13. A. Nadort, K. Kalkman, T. G. van Leeuwen, and D. J. Faber, "Quantitative blood flow velocity imaging using laser speckle flowmetry," *Sci. Rep.* **6**(1), 25258 (2016).
14. P. J. Marchand, D. Szlag, A. Bouwens, and T. Lasser, "In vivo high-resolution cortical imaging with extended-focus optical coherence microscopy in the visible-NIR wavelength range," *J. Biomed. Opt.* **23**(3), 1–7 (2018).
15. H. Ojima, M. Takayanagi, D. Potapov, and R. Homma, "Isofrequency Band-like Zones of Activation Revealed by Optical Imaging of Intrinsic Signals in the Cat Primary Auditory Cortex," *Cereb. Cortex* **15**(10), 1497–1509 (2005).
16. Y. B. Sirotin, E. M. C. Hillman, C. Bordier, and A. Das, "Spatiotemporal precision and hemodynamic mechanism of optical point spreads in alert primates," *Proc. Natl. Acad. Sci. U.S.A.* **106**(43), 18390–18395 (2009).
17. S. Kawai, Y. Takagi, S. Kaneko, and T. Kurosawa, "Effect of Three Types of Mixed Anesthetic Agents Alternate to Ketamine in Mice," *Exp. Anim.* **60**(5), 481–487 (2011).
18. S. Zhang and T. H. Murphy, "Imaging the impact of cortical microcirculation on synaptic structure and sensory-evoked hemodynamic responses in vivo," *PLoS Biol.* **5**(5), e119 (2007).
19. R. J. Nudo, "Recovery after brain injury: mechanisms and principles," *Front. Hum. Neurosci.* **7**, 887 (2013).
20. A. Y. Shih, N. Nishimura, J. Nguyen, B. Friedman, P. D. Lyden, C. B. Schaffer, and D. Kleinfeld, "Optically induced occlusion of single blood vessels in rodent neocortex," *Cold Spring Harb. Protoc.* **2013**(12), 1153–1160 (2013).
21. Y. Kurauchi, K. Mokudai, A. Mori, K. Sakamoto, T. Nakahara, M. Morita, A. Kamimura, and K. Ishii, "l-Citrulline ameliorates cerebral blood flow during cortical spreading depression in rats: Involvement of nitric oxide- and prostanoids-mediated pathway," *J. Pharmacol. Sci.* **133**(3), 146–155 (2017).